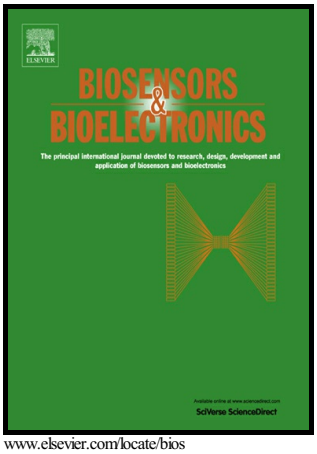

www.elsevier.com/locate/bios

An electrochemical impedance biosensor for Hg^{2+} detection based on DNA hydrogel by coupling with DNAzyme-assisted target recycling and hybridization chain reaction

Wei Cai, Shunbi Xie, Jin Zhang, Dianyong Tang, Ying Tang

PII: S0956-5663(17)30475-X
DOI: http://dx.doi.org/10.1016/j.bios.2017.07.025
Reference: BIOS9858

To appear in: *Biosensors and Bioelectronic*

Received date: 8 May 2017
Revised date: 6 July 2017
Accepted date: 10 July 2017

Cite this article as: Wei Cai, Shunbi Xie, Jin Zhang, Dianyong Tang and Ying Tang, An electrochemical impedance biosensor for Hg^{2+} detection based on DNA hydrogel by coupling with DNAzyme-assisted target recycling and hybridization chain reaction, *Biosensors and Bioelectronic* http://dx.doi.org/10.1016/j.bios.2017.07.025

An electrochemical impedance biosensor for Hg^{2+} detection based on DNA hydrogel by coupling with DNAzyme-assisted target recycling and hybridization chain reaction

Wei Cai, Shunbi Xie*, Jin Zhang, Dianyong Tang, Ying Tang*

Chongqing Key Laboratory of Environmental Materials and Remediation Technologies (Chongqing University of Arts and Sciences), Chongqing University of Arts and Sciences, Chongqing 402160, PR China

xieshunbi@163.com

tangying@cqwu.edu.cn

* Corresponding author. Tel.: +86-23-49891739

Abstract

In this work, an electrochemical impedance biosensor for high sensitive detection of Hg^{2+} was presented by coupling with Hg^{2+}-induced activation of Mg^{2+}-specific DNAzyme (Mg^{2+}-DNAzyme) for target cycling and hybridization chain reaction (HCR) assembled DNA hydrogel for signal amplification. Firstly, we synthesized two different copolymer chains P1 and P2 by modifying hairpin DNA H3 and H4 with acrylamide polymer, respectively. Subsequently, Hg^{2+} was served as trigger to activate the Mg^{2+}-DNAzyme for selectively cleavage ribonucleobase-modified substrate in the presence of Mg^{2+}. The partial substrate

strand could dissociate from DNAzyme structure, and hybridize with capture probe H1 to expose its concealed sequence for further hybridization. With the help of the exposed sequence, the HCR between hairpin DNA H3 and H4 in P1 and P2 was initiated, and assembled a layer of DNA cross-linked hydrogel on the electrode surface. The formed non-conductive DNA hydrogel film could greatly hinder the interfacial electronic transfer which provided a possibility for us to construct a high sensitive impedance biosensor for Hg^{2+} detection. Under the optimal conditions, the impedance biosensor showed an excellent sensitivity and selectivity toward Hg^{2+} in a concentration range of 0.1 pM - 10 nM with a detection limit of 0.042 pM. Moreover, the real sample analysis reveal that the proposed biosensor is capable of discriminating Hg^{2+} ions in reliable and quantitative manners, indicating this method has a promising potential for preliminary application in routine tests.

Keywords: mercury ions, Mg^{2+}-specific DNAzyme, hybridization chain reaction, DNA hydrogel, impedance biosensor

1. Introduction

Mercuric ion (Hg^{2+}) is one of notorious pollutants for its widespread and highly toxic, and has been reported to pose severe adverse effects on human health and environmental even relatively low concentration (Ren et al., 2016; Wang et al., 2014). In the past decades, mercury contamination has been a critical issue of concern throughout the whole word (Bridges et al., 2017). The water-soluble Hg^{2+}, the most prevalent forms of mercury contamination, is generally considered to be one of the

most toxic forms because it could preferentially bind to thiol-containing molecules and accumulate in human body by food chain (Vázquez et al., 2015; Bridges et al., 2015; Zeng et al., 2014). Therefore, the development of high sensitive sensors for Hg^{2+} detection is of great significance in food monitoring and environmental protection, as well as clinical toxicology (Liu et al., 2009). In the past few years, various fluorescence and colorimetric strategies based on carbon materials (Huang et al., 2014a; Cui et al., 2015; Zhang et al., 2014a; Wang et al., 2014), metal nanoparticles (Tang et al., 2015; Dasari et al., 2014; Wu et al., 2014), semiconductor quantum dots (Zhang et al., 2014b), polymer materials (Childress et al., 2012; Tan et al., 2012) and Ag/Hg amalgam (Deng et al., 2013) for Hg^{2+} detection have been reported. Unfortunately, most of them were limited by poor water solubility, insufficient sensitivity or inferior selectivity. Therefore, the demand for designing highly sensitive and selective sensors for Hg^{2+} analysis has urgently risen.

In recent years, using exquisite biological components to fabricate metal ions sensing platform gradually became one of the predominant strategies. DNAzyme, an enzyme-free amplification technique, has garnered great attention in fabrication of sensors owing to its high catalytic efficiency, versatility and designability (Huang et al., 2014b; Huang et al., 2016). For example, ions-dependent DNAzyme has been extensively used as an amplifying label for fluorescent or colorimetric detection of DNA (Wang et al., 2011; Wang et al., 2013; Johann et al., 2009) or heavy metal ions (Zhang et al., 2013; Bi et al., 2010; Aleman-Garcia et al., 2014). Another brilliant methodology for Hg^{2+} sensing was thymine-Hg^{2+}-thymine (T-Hg^{2+}-T) coordination

chemistry. Since Ono (Ono et al., 2004) and Miyake (Miyake et al., 2006) demonstrated that Hg^{2+} has highly affinity with T-T mismatch base pairs in oligonucleotides, the T-Hg^{2+}-T coordination chemistry has been served as a selective and versatile strategy for Hg^{2+} detection. Although numerous of detection systems based on DNAzyme or T-Hg^{2+}-T have been used to fabrication of sensors, there are only a few reports concerning Hg^{2+} detection by incorporating T-Hg^{2+}-T coordination chemistry into DNAzyme. Recently， some fluorescent sensing systems that combining DNAzyme with T-Hg^{2+}-T coordination chemistry for Hg^{2+} detection were designed. For example, Shimron and co-workers developed a reversible switch based on T-Hg^{2+}-T coordination chemistry induced activation the Mg^{2+}-dependent DNAzyme for Hg^{2+} detection (Shimron et al., 2010). Li's groups designed a fluorescent sensing system based on T-Hg^{2+}-T triggered formation of three-way Mg^{2+}-dependent DNAzyme for the detection of Hg^{2+} and with a limit of detection of 4.5 pM (Li et al., 2017). On the basis of these works, we attempted to utilize this methodology to construct an electrochemical biosensor for the sensitive detection of Hg^{2+} by employing the advantages of electrochemical such as sensitivity, low cast, rapid detection and simplicity.

DNA hydrogel, a porous 3D network polymer containing a large fraction of water, was constructed by the crosslinking of nucleic acid-tethered polymer chains that have attracted immense interest in materials science (Hu et al., 2016; Guo et al., 2014). Owning its large loading capacity, mechanical stability, biodegradability, high biocompatibility and stimuli-responsive, DNA hydrogel have been wildly applied in

functional materials (Hu et al., 2016; Zinchenko et al., 2014; Guo et al., 2015), biocatalysis (Lilienthal et al., 2015), biomedicine (Soontornworajit et al., 2010; Bi et al., 2015) and sensors (Huang et al., 2016; Huang et al., 2014c; Liu et al., 2015). Although the application of DNA hydrogel has been involved in various fields, the use of DNA hydrogel as an electrochemical signal amplification element to fabricate sensing platform for metal ions detection was barely reported. Recently, Gibbs's group has developed an electrochemical detection system based on assembling a layer of ferrocenyl modified polymer-DNA hybrids on electrode surface for the amplified detection of DNA (Gibbs et al., 2005). Kahn's and co-workers designed a switchable electrocatalytic film based on self-assemble DNA copolymer hydrogel on gold-coated surface through hybridization chain reaction (HCR) (Kahn et al., 2015). Yang et al constructed an impedimetric aptasensor based on target-triggered pH-stimulated DNA hydrogel for heparanase detection by taking use of the interfacial electron transfer properties of hydrogel (Yang et al., 2017). Inspired by those reports, we designed an electrochemical impedance biosensor based on self-assemble a layer of DNA hydrogel *via* HCR on the electrode surface as a signal amplification element for Hg^{2+} detection.

Herein, we combine the Hg^{2+}-induced activation of Mg^{2+}-specific DNAzyme with the HCR between two hairpin-modified polymer chains to introduce a layer of DNA hydrogel on the electrode for Hg^{2+} sensing. As shown in scheme 1B, The Mg^{2+}-specific DNAzyme consist of subunits D1 and D2 (the pink domain is rich in T bases). When Hg^{2+} ions are added with certain concentration, the pink domain of the

DNAzyme subunits D1 and D2 are tethered to form inter-nucleic acid T-Hg^{2+}-T complexes, which can assemble on ribonuclease-modified hairpin probe H2 (H2) loop to yield an inactive DNAzyme structure. In the presence of Mg^{2+}, the DNAzyme has been activated, and cleaved substrate at the ribonuclease site to release single-DNA (sDNA) and inter-nucleic acid T-Hg^{2+}-T complexes. The released inter-nucleic acid T-Hg^{2+}-T complexes are available for next cleavage process, which can generate large quantities of sDNA after cyclic process. When the produced sDNA are incubated on hairpin probe H1 (H1) modified electrode, the hairpin structure of H1 will be opened and exposed its concealed sequence. Then, the exposed sequences of H1 are served as initiators to trigger HCR between P1 and P2, leading to polyacrylamide chains layer-by-layer assemble on the electrode surface. As a result, the interfacial electron transfer properties are significant affected by the DNA hydrogel. Thus, the content of the Hg^{2+} can be easily analyzed with high sensitive by combining DNAzyme-assisted target cycling with DNA hydrogel-induced signal amplification. The detection principle of the proposed biosensor is shown in scheme 1.

2. Experiment

2.1 Materials and reagents

Tris(hydroxymethyl)aminomethane (Tris), magnesium chloride, sodium chloride, potassium chloride, calcium chloride were obtained from Titan Scientific Co., Ltd. (Shanghai, China). 4-(2-hydroxyethyl)-1-piperazineethanesulfonic acid (HEPES), ammonium persulfate (APS), *N*,*N*,*N*′,*N*′-tetramethylethylenediamine (TEMED) and

acrylamide solution (40%) were provided by Sangon biotech Co., Ltd. (Shanghai, China). Tris(2-carboxyethyl)phosphine (TCEP), 6-mercapto-1-hexanol (MCH) and gold chloride ($HAuCl_4$) were purchased from Sigma-Aldrich (St, Louis, MO, U.S.A). Hg^{2+} standard solution was obtained by National Center of Analysis and Testing for Nonferrous Metals and Electronic Materials (Beijing, China). All other chemical regents are analytical grade and without any purification before using.

Buffers employed in this work were listed as follows. Binding buffer: 10 mM Tris-HCl buffer (pH 8.0) containing 140 mM NaCl, 5 mM KCl, 1 mM $CaCl_2$ and 1 mM $MgCl_2$. Coating buffer (pH 7.2): 25 mM HEPES and 100 mM NaCl. HEPES buffer (pH 7.2): 25 mM HEPES, 1 M $NaNO_3$ and 20 mM $Mg(Ac)_2$. HCR buffer (pH 7.2): 25 mM HEPES and 25 mM $MgCl_2$. 5 × TBE buffer (pH 8.0): 445 mM Tris base, 445 mM boric acid and 10 mM EDTA. Electrochemical impedance spectroscopy testing buffer (E-buffer: a volume ratio of 1 : 1 mixture of 25 mM HCR buffer and 2 mM $Fe(CN)_6^{3-/4-}$). All the oligonucleotides were synthesized and purified by Sangon biotech Co., Ltd. (Shanghai, China) and listed in Table 1.

2.2 Apparatus and measurements

The morphology of DNA hydrogel was recorded by scanning electrode microscope (SEM, S-4800, Hitachi, Japan). All electrochemical measurements, including cyclic voltammetry (CV) and electrochemical impedance spectroscopy (EIS) were carried out on a CHI 660E electrochemical workstation (Shanghai Chenhua instrument, China) with a conventional three-electrode system: a modified glass

carbon electrode (GCE, Φ = 3 mm) as working electrode, a platinum wire and Ag/AgCl (saturated with KCl) were served as counter electrode and reference electrode, respectively. CV measurements were carried out in 2 mL of $[Fe(CN)_6]^{3-/4-}$ (5.0 mM) containing 0.1 M KCl with potential range from -0.2 to 0.6 V at a scan rate of 50 mV s^{-1}. Electrochemical impedance spectroscopy (EIS) experiments were recorded in E-buffer, with the potential of 0.272 V (versus Ag/AgCl), the amplitude of 5 mV and the frequency range from 0.1 Hz to 10^5 Hz.

2.3 Synthesis of DNA-modified polyacrylamide chains

The polyacrylamide/DNA copolymers were synthesized according to the previous reports (Guo et al., 2015; Kahn et al., 2015). The synthesis process was shown in scheme 1A, as the acrydite modification just occurred at the 5′ end of DNA, we used a short acrydite-modified DNA (A1) strand to tether H4 for synthesis of P2. The synthesis details were as follows, 20 μL of H3 (100 μM) and 20 μL of A1 (100 μM) were separately added into 80 μL of 10 mM binding buffer that include 2% (*w/v*) acrylamide. After the as-mixed monomer solution was bubbled with nitrogen gas for 5 min, a freshly prepared initiator, 100 μL aqueous solution containing 10 mg APS and 5 μL TEMED, was separately added into the mixture at 1.4% volumetric ratio with nitrogen bubbling for another 5 min. Then, the mixture was incubated at 4 ˚C for 12 hours to further polymerize. To remove all of the unpolymerized strands, acrylamide monomer, salts and initiator, the polymer P1 and A1-modified polymer (P_{A1}) were filtered through a MWCO 30 kDa and 10 kDa columns, respectively. After that, the resulting-polymers were rinsed with water three times, and the final rinse was

conducted by HCR buffer. And then, the polymer-incorporated H4 was added in P_{A1} with a 1:1 molar ratio for forming the polymer P2. Then, P1 and P2 were incubated at 95 ˚C for 5 minutes, followed immediately cooled by 30 min ice incubation to ensure sufficient formation of hairpin structure. After that, the prepared polymers were stored in 4 ˚C for further use.

2.4 *DNAzyme assays*

The Hg^{2+}-induced activation of Mg^{2+}-specific DNAzyme system was designed according the previous work (Shimron et al., 2010). As shown in scheme 1B, the 100 μL HEPES buffer solution that consisted of D1 (4 μM), D2 (4 μM) and H2 (4 μM) and variable concentrations of Hg^{2+} was heated to 95 °C for 5 min, followed gradually cooled down to room temperature. After that, the resulting mixture was stored in 4 °C for further use.

2.5 Fabrication of the electrochemical biosensor

First of all, 100 μL of coating buffer including 4 μM thiolated H1 and 5 mM TCEP was incubated 30 min to reduce the formation of disulfide bonds, and then the mixture was annealed at 95 °C for 5 min and further slowly cooled to room temperature. To obtain a mirror-like surface, GCE was polished with 0.3 and 0.05 μm alumina slurries and rinsed thoroughly with ultrapure water, and then sequential sonication in water, ethanol and water for 5 min. After that, a layer of AuNPs was obtained by soaking the electrode in $HAuCl_4$ solution (1% *w*/*w*) for electrodeposition 30 s under the potential of -0.20 V. Then, 8 μL of H1 (4 μM) was dropped on the surface of AuNPs/GCE, and incubated for 14 h at room temperature for

self-assembling of H1 on the gold surface. After rinsing thoroughly with ultrapure water, 8 μL of MCH (2.0 mM) was employed to block the non-active sites for 30 min. Then, the electrode was washed thoroughly by ultrapure water for three times to avoid a stronger background signal. Subsequently, 8 μL of the DNAzyme hydrolytic products (DHPs) were incubated on the electrode for 2 h at 37 °C to perform hybridization reaction between sDNA and H1. After the hybridization, 8 μL of the prepared polymer chains P1 and P2 were immediately mixed, and placed on the electrode for another 2 h at 37 °C to form the DNA-hydrogel. After that, the DNA-hydrogel based biosensor was carried out.

2.6 Gel electrophoresis analysis

The feasibility of HCR was analyzed by 16% non-denaturing polyacrylamide gel electrophoresis (PAGE). The gel was run at 120 V for 110 min in 1 × TBE buffer and stained by 4S Green for 30 min. The image of the electrophoresis was recorded by Tanon 5200 Multi Chemiluminescent/Fluorescence Image System.

3. Results and discussion

3.1 Electrochemical characterization of biosensor

To characterize the behavior of the fabrication and assembly process of the biosensor, electrochemical impedance spectroscopy (EIS) was employed as a tool to monitor the interfacial properties of each modified step. The inset of Figure 1A represented the Randle equivalent circuit, which was used to fit the EIS data by using the ZSimpWin software. The equivalent circuit includes charge transfer resistance (R_{ct}), the capacitance (C_{dl}), electrolyte resistance (R_s) and Warburg element (Z_w). In

the Nyquist plot, the R_{ct}, directly controls the transfer kinetics of the redox-probe electron at the electrode surface, corresponds to the diameter of the semicircle (Hou et al., 2014a, 2014b). As shown in Figure 1A, the bare GCE shows a small semicircle in the impedance spectra ($R_{ct} \approx 324.2$ Ω, curve a). After the AuNPs was electrodeposited on the bare GCE, the semicircle almost decreased into a liner plot in the impedance spectra (curve b). This result is attributed to the deposition of AuNPs possess excellent electrical conductivity. When H1 was assembled on the electrode, the semicircle increased a lot ($R_{ct} \approx 516$ Ω, curve c). This increased mainly attributes to the accumulation of negatively charged probe H1 which introduce much stronger steric hindrance and electrostatic repulsion to the diffusion process of redox probe $[Fe(CN)_6]^{3-/4-}$ toward the electrode surface (Kjallman et al., 2008; Tripathya et al., 2017). With the nonspecific sites blocked by the inert MCH, the semicircle was further increase ($R_{ct} \approx 876.2$ Ω, curve d). After the subsequently incubation of the DHPs on the electrode, the diameter of the semicircle increased again ($R_{ct} \approx 1274.4$ Ω, curve e). This increase mainly derives from the hybridization of sDNA and H1, and formed duplex DNA on the electrode surface. Finally, when the acrylamide copolymer chain was incubated on the electrode, a significantly increased semicircle could be observed ($R_{ct} \approx 3186.3$ Ω, curve f). This phenomenon might be the fact that the HCR-induced surface-formed a layer of insulating polymer film that consisted of negatively charged duplex DNA and acrylamide polymer, which could effectively obstruct the electron transfer/repel the redox probe diffusing to the electrode surface.

Moreover, the cyclic voltammetry (CV) was also employed to characterize the

stepwise fabrication process of the proposed biosensor. As shown in Figure 1B, a pair of well-defined redox peak of $[Fe(CN)_6]^{3-/4-}$ was observed at the bare GCE electrode (curve a). After the AuNPs were deposited on the electrode, the peak current was significantly increased (curve b). When the negatively charged H1 was assembled onto the AuNPs modified electrode, the peak was decreased again (curve c). After the non-electroactive MCH was adopted to block the nonspecific sites of the electrode, the peak current was decreased consecutively (curve d). With incubation of the DHPs, the peak current was further decreased (curve e). Finally, the mixture of acrylamide copolymer chain P1 and P2 was incubated on the electrode to form DNA hydrogel, the peak current decreased obviously (curve f). These results were consistent with the above EIS results. Thus, we might make a preliminary conclusion that the proposed biosensor based on DNA hydrogel was successfully prepared.

3.2 Investigation DNA hydrogel formed by HCR

In this study, the DNA hydrogel formation was realized though self-assemble DNA-modified polyacrylamide chains by HCR. To determine the feasibility of HCR, we used gel electrophoresis to analyze the reaction process. Prior to experiment, the DNAzyme system and other hairpin structure DNA were annealed. The lanes 1-8 were loaded with the DHPs, H3, H4/A1, H1, DHPs hybridize with H1 (HPs1), DHPs and H1 hybridize with H3 (HPs2; note that the H3 used here exceed DHPs and H1), DHPs and H1 hybridize with H4/A1, the HCR products, respectively. As Figure S1 illustrated (see supporting information), the hairpin probe H1 exhibited a clearly band

with the negligible byproduct strand (lane 4). When H1 of the same concentration was added into DHPs, a sharp and neat band was found (lane 5), which indicated that the loop region of hairpin H1 was opened by the DHPs and formed duplex strand DNA. By introducing H3 to the mixture of H1 and DHPs, an obvious band was obtained (lane 6), consisting of bands matched with the lane 2 and lane 5, which demonstrated that the hairpin structure of H3 was opened by the initiator sequences. As a sharp contrast, even if the high concentration of H4/A1 was introduced into the H1 and DHPs mixture, there is no obvious band observed (lane 7), demonstrating the hybridization between the initiator sequences of HPs1 and H4/A1 dose not happened. When H3 and H4/A1 were introducing into the mixture of H1 and DHPs, several bright bands could be observed at the lane top (lane 8). These results showed that the design of this work was successful.

To further validate that the DNA-hydrogel was formed through the HCR between P1 and P2, the performance of the sDNA-modified gold electrode treated with different processes were investigated. The evaluation was based on the change of resistance relative to the sDNA-modified electrode (ΔR_{ct}, where $\Delta R_{ct} = R_1 - R_0$). As shown in Figure S2, comparing with curves a ($R_{ct} \approx 1310\ \Omega$), the resistance increased a little when the electrode just incubated with P1 (curves b, $\Delta R_{ct} \approx 530\ \Omega$). This phenomenon might be attribute to the hairpin structure of H3 in P1 could be opened by the residue sequence of sDNA, and formed a double-strand DNA left on the electrode. While, when the modified electrode incubated with P2 only, the resistance

did not have any notable increase (curves c, $\Delta R_{ct} \approx 90\ \Omega$). We speculate that the loop of the hairpin H4 in P2 cannot be opened by the residue sequence of sDNA. However, when the mixture of P1 and P2 was incubated on the electrode, a dramatic increase of the resistance was found (curves d, $\Delta R_{ct} \approx 2020\ \Omega$). This increase may be attribute to the polyacrylamide/DNA copolymer film was formed on the electrode by HCR.

3.3 characterization of DNA hydrogel on surface

The morphology of the DNA hydrogel was recorded by scanning electron microscope (SEM). To obtain the porous network structure, a fresh prepared DNA hydrogel were placed on a undefiled silicon slide surface, and then immersed in liquid nitrogen and dried by sublimation of the generated ice crystals under vacuum (Guo et al., 2015; Kahn et al., 2015). As shown in Figure S3 (see supporting information), a irregularly porous network structure would be observed, indicating that the DNA hydrogel was prepared successfully.

3.4 Contribution of DNA hydrogel on signal amplification

The mainly concern of the proposed impedance biosensor is the contribution of the DNA hydrogel on signal amplification. To demonstrate this point, the sDNA modified electrode was used to detection of 1 nM Hg^{2+} by treating with different amplification strategies. The effect of the DNA hydrogel on signal amplification was evaluated by the change of resistance relative to the sDNA-modified electrode (ΔR_{ct}, where $\Delta R_{ct} = R_1 - R_0$). As seen from Figure 2, the resistance of sDNA-modified

electrode was about 1230 Ω (curves a). With the mixture of H3 and H4/A1 incubated on the sDNA modified electrode, only a relative low increase in the resistance was observed (Figure 2A, $\Delta R_{ct} \approx 1010$ Ω). However, when the electrode was treated with the mixture of P1 and P2, the resistance was significantly increased (Figure 2B, $\Delta R_{ct} \approx 2160$ Ω). This reason might be attribute to the HCR-induced form a layer of DNA hydrogel on the electrode, which could effectively hinder the diffusion of ferricyanide ions to the electrode surface. Those results indicated that the nucleic acid cross-linked acrylamide hydrogel plays an important role in improving the impedimetric signal.

3.5 Optimization of hybridization time

The hybridization time of the HCR was an important parameter in the DNA hydrogel formation. To achieve an optimum analytical performance of the detection system, the hybridization time of the HCR was optimized. Figure S4 showed the effect of different hybridization time of HCR on the impedimetric response. With the prolongation of the hybridization time, the resistance increased obviously. However, we could not observe a distinct change in the resistance after the hybridization time excess over 120 min. Hence, 120 min was selected as the optimized hybridization time of the HCR in the following work.

3.6 Electrochemical measurement of Hg^{2+}

To evaluate the analytical performance of the proposed biosensor, the resistance changes of the detection system was recorded by analyzing a series of Hg^{2+}

concentrations (from 0.1 pM to 10 nM) under the optimal conditions. As displayed in Figure 3A, the semicircle domain increased proportionally with the increase of Hg^{2+} concentration in the dynamic range of 0.1 pM to 10 nM. Figure 3B showed the linear dependence between the resistance and the logarithm Hg^{2+} concentration in the range of 0.1 pM to 10 nM with a detection limit (LOD) of 0.042 pM (evaluated from signal-to-noise ratio of 3σ, where σ is the standard deviation of a blank sample, n = 11). The linear regression equation was obtained as R_{ct} = 393.16 $\lg c_{Hg^{2+}}$ (nM) + 3285.30 with the correlation coefficient of r = 0.9985. In addition, we also made a comparison of the performance of this method with some existed detection schemes, which was listed in Table S1. As seen from the Table S1, the sensitivity of our strategy was better than the previously reported methods.

3.7 Reproducibility and selectivity

To investigate the reproducibility and precision of the prepared biosensor, we evaluated three different Hg^{2+} levels of the intra-assay and inter-assay, such as 1 pM, 10 pM and 100 pM. The experimental results revealed that the relative standard deviations (RSD) toward the mentioned-above concentration of the intra-assay were 5.6%, 4.9%, 4.1% and the inter-assay were 7.8%, 7.4%, 6.8% (n = 3). Therefore, the reproducibility and the precision of the proposed biosensor were acceptable. The selectivity of the proposed biosensor for Hg^{2+} detection was evaluated by using the commonly present metal ions in the environment (e.g. Ag^{+}, Mn^{2+}, Al^{3+}, Ba^{2+}, Cu^{2+}, Co^{2+}, Cd^{2+}, Ni^{2+} and Fe^{3+}) to substitute the target Hg^{2+}. As seen from Figure 4, the

specific target Hg^{2+} (1 nM) produced a dramatic higher resistance relative to the blank sample, while the interferential metal ions only led to a slight change, even of high concentration (10 nM), indicating the good selectivity of the development biosensor in this study.

3.8 Practical application

In order to investigate whether this impedimetric sensing system could be applied to real samples, a recovery experiment was carried out. The tap water samples, obtained from the tap in our laboratory, were spiked with different concentrations of Hg^{2+}. As shown in Table 2, the recovery and RSD were range from 95.2% to 103.3% and 3.2% to 6.8% (n = 3), respectively. This result indicated that our method not only holds quite high accuracy, but also could be preliminarily employed for Hg^{2+} detection in tap water.

4. Conclusions

In summary, a DNA hydrogel-based electrochemical impedance biosensor for Hg^{2+} detection was successful developed. In this study, Hg^{2+}-induced activation Mg^{2+}-DNAzyme was served as target cycling amplification strategy to initiate the HCR for introducing surface-confined hydrogel films. This approach takes advantage of the native composition and structure of the DNA hydrogel, and served it as a signal amplification element, which could effectively enhance EIS response to realize high sensitive detection of Hg^{2+}. Meanwhile, the sensitivity of this method was also

improved by the DNAzyme-assisted target recycling. Moreover, the selectivity of the biosensor was guaranteed by the specific bonding of Hg^{2+} to T bases, which could discriminate Hg^{2+} toward other interferential metal ions. In addition, the recovery experiments reveal that the proposed biosensor has a great potential to discriminate Hg^{2+} ions in complex river water samples with a reliable and quantitative manner.

Acknowledgements

This work was financially supported by the Chongqing Science and Technology Commission of China (cstc2015jcyjBX0126, cstc2016shmsZX20001, cstc2017jcyjAX0282), the Science and Technology Research Program of Chongqing Municipal Education Commission of China (KJ1711265), Chongqing University of Arts and Sciences, China (R2016CH08).

References

Aleman-Garcia, M. A., Orbach, R., Willner, I., 2014. Chem. Eur. J. 20, 5619-5624.

Bi, S., Xiu, B., Ye, J. Y., Dong, Y., 2015. ACS Appl. Mater. Interfaces 7, 23310-23319.

Bi, S., Yan, Y. M., Hao, S. Y., Zhang, S. S., 2010. Angew. Chem. Int. Ed. 122, 4540-4544.

Bridges, C. C., Zalups, R. K., 2017. Arch. Toxicol. 91, 63-81.

Bridges, C. C., Zalups, R. K., Joshee, L., 2015. Toxicol. Appl. Pharm. 285, 110-117.

Childress, E. S., Roberts, C. A., Sherwood, D. Y., LeGuyader, C. L. M., Harbron, E. J., 2012. Anal. Chem. 84, 1235-1239.

Cui, X., Zhu, L., Wu, J., Hou, Y., Wang, P. Y., Wang, Z. N., Yang, M., 2015. Biosens. Bioelectron. 63, 506-512.

Dasari, R., Tai, K., Robinson, D. A., Stevenson, K. J., 2014. ACS Nano 8, 4539-4546.

Deng, L., Ouyang, X. Y., Jin, J. Y., Ma, C., Jiang, Y., Zheng, J., Li, J. S., Li, Y. H., Tan, W. H., Yang, R. H., 2013. Anal. Chem. 85, 8594-8600.

Gibbs, J. M., Park, S. J., Anderson, D. R., Watson, K. J., Mirkin C. A., Nguyen. S. T., 2005. J. Am. Chem. Soc. 127, 1170-1178.

Guo, W. W., Lu, C. H., Orbach, R., Wang, F., Qi, X. J., Cecconello, A., Seliktar, D., Willner, I., 2015. Adv. Mater. 27, 73-78.

Guo, W. W., Qi, X. J., Orbach, R., Lu, C. H., Freage, L., Mironi-Harpaz, I., Seliktar, D., Yang, H. H., Willner, I., 2014. Chem. Commun. 50, 4065-4068.

Hou, L., Gao, Z. Q., Xu, M. D., Cao, X., Wu, X. P., Chen, G. N, Tang, D. P., 2014a. Biosens. Bioelectron. 54, 365-371.

Hou, L., Tang, Y., Xu, M. D., Gao, Z. Q., Tang, D. P., 2014b. Anal. Chem. 86, 8352-8358.

Hu, Y. W., Guo, W. W., Kahn, J. S., Aleman-Garcia, M., A., Willner, I., 2016. Angew. Chem. Int. Ed. 55, 4210-4214.

Huang, J. H., Gao, X., Jia, J. J., Kim, J. K., Li, Z. G., 2014a. Anal. Chem. 86, 3209-3215.

Huang, P. J. J., Liu, J. W., 2014b. Anal. Chem. 86, 5999-6005.

Huang, Y. S., Fang, L. T., Zhu, Z., Ma, Y. L., Zhou, L. J., Chen, X., Xu, D. M., Yang, C. Y., 2016. Biosens. Bioelectron. 85, 496-502.

Huang, Y. S., Ma, Y. L., Chen, Y. H., Wu, X. M., Fang, L. T., Zhu, Z., Yang, C. Y., 2014c. Anal. Chem. 86, 11434-11439.

Johann, E., Michal, M., Bella, S., Itamar, W., 2009. Chem. Eur. J. 15, 3411-3418.

Kahn, J. S., Trifonov, A., Cecconello, A., Guo, W. W., Fan, C. H., Willner, I., 2015. Nano Lett. 15, 7773-7778.

Kjallman, T. H. M., Peng, H., Soeller, C., Travas-Sejdic, J., 2008. Anal. Chem. 80, 9460-9466.

Li, X., Xie, J. Q., Jiang, B. Y., Yuan, R., Xiang, Y., 2017. ACS Appl. Mater. Interfaces 9, 5733-5738.

Lilienthal, S., Shpilt, Z., Wang, F., Orbach, R., Willner, I., 2015. ACS Appl. Mater. Interfaces 7, 8923-8931.

Liu, R. D., Huang, Y. S., Ma, Y. L., Jia, S. S., Gao, M. X., Li, J. X., Zhang, H. M., Xu, D. M., Wu, M., Chen, Y., Zhu, Z., Yang, C. Y., 2015. ACS Appl. Mater. Interfaces 7, 6982-6990.

Liu, S. J., Nie, H. G., Jiang, J. H., Shen, G. L., Yu, R. Q., 2009. Anal. Chem. 81, 5724-5730.

Miyake Y., Togashi, H., Tashiro, M., Yamaguchi, H., Oda, S., Kudo, M., Tanaka, Y., Kondo, Y., Sawa, R., Fujimoto, T., Machinami, T., Ono, A., 2006. J. Am. Chem. Soc. 128, 2172-2173.

Ono, A., Togashi, H., 2004. Angew. Chem. Int. Ed. 43, 4300-4302.

Ren, W., Zhang, Y., Chen, H. G., Gao, Z. F., Li, N. B., Luo, H. Q., 2016. Anal. Chem. 88, 1385-1390.

Shimron, S., Elbaz, J., Henning A., Willner, I., 2010. Chem. Commun. 46, 3250-3252.

Soontornworajit, B., Zhou, J., Zhang, Z., Wang, Y., 2010. Biomacromolecules 11, 2724.

Tan, H. L., Liu, B. X., Chen, Y., 2012. ACS Nano 6, 10505-10511.

Tang, S. R., Tong, P., Wang, M. L., Chen, J. H., Li, G. W., Zhang, L., 2015. Chem. Commun. 51, 15043-15046.

Tripathya, S., Vanjaria, S. R. K., Singh, V., Swaminathan, S., Singh, S. G., 2017. Biosens. Bioelectron. 90, 378-387.

Vázquez, M., Vélez, D., Devesa, V., Puig, S., 2015. Toxicology 331, 119-124.

Wang, F., Elbaz, J., Teller, C., Willner, I., 2011. Angew. Chem. Int. Ed. 50, 295-299.

Wang, F., Freage, L., Orbach, R., Willner, I., 2013. Anal. Chem. 85, 8196-8203.

Wang, G. F., Xu, G., Zhu, Y. H., Zhang, X. J., 2014. Chem. Commun. 50, 747-750.

Wu, G. W., He, S. B., Peng, H. P., Deng, H. H., Liu, A. L., Lin, X. H., Xia, X. H., Chen, W., 2014. Anal. Chem. 86, 10955-10960.

Yang, Z. H., Zhuo, Y., Yuan, R., Chai, Y. Q., 2017. Nanoscale 9, 2556-2562.

Zeng, T., Li, T., Li, Y. R., Liu, L., Wang, X. Y., Liu, Q. S., Zhao, Y. L., Wu, H. C., 2014. Nanoscale 6, 8579-8584.

Zhang, H., Jia, S. S., Lv, M., Shi, J. Y., Zuo, X. L., Su, S., Wang, L. H., Huang, W., Fan, C. H., Huang, Q., 2014a. Anal. Chem. 86, 4047-4051.

Zhang, J., Yu, S. H., 2014b. Nanoscale 6, 4096-4101.

Zhang, L., Zhang, Y. M., Liang, R. P., Qiu, J. D., 2013. J. Phys. Chem. C 117, 12352-12357.

Zinchenko, A., Miwa, Y., Lopatina, L. I., Sergeyev, V. G., Murata, S., 2014. ACS Appl. Mater. Interfaces 6, 3226-3232.

Scheme 1. Schematic illustration of the impedance biosensor based on DNA-hydrogel for sensitive detection of Hg^{2+}.

Figure 1. EIS (A) and CV (B) responses of the biosensor stepwise fabrication process in 2 mL of E-buffer and 5 mM $Fe(CN)_6^{3-/4-}$, respectively. (a) bare GCE; (b) AuNPs/GCE; (c) H1/AuNPs/GCE; (d) MCH/H1/AuNPs/GCE; (e) sDNA/MCH/H1/AuNPs/GCE; (f) DNA hydrogel/sDNA/MCH/H1/AuNPs/GCE.

Figure 2. The EIS responses of the sDNA/MCH/H1/AuNPs/GCE treated with (A) H3 and H4/A1, (B) P1 and P2, respectively. [Note: Curve a stands for the impedance response of sDNA/MCH/H1/AuNPs/GCE, whereas curve b represents the control experiments.]

Figure 3. EIS for Hg^{2+} detection at various concentrations: (a) blank; (b) 0.1 pM; (c) 1 pM; (d) 10 pM; (e) 100 pM; (f) 1 nM; (g) 5 nM; (h) 10 nM. (B) The linear relationship between the R_{ct} and the logarithm of Hg^{2+} concentration.

Figure 4. Selectivity of the impedimetric sensor towards different interferences: Ag^{+}, Mn^{2+}, Al^{3+}, Ba^{2+}, Cu^{2+}, Co^{2+}, Cd^{2+}, Ni^{2+} and Fe^{3+}. The concentration of each metal ion was 10 nM.

Table 1. Sequences of the oligonucleotides used in this work.

Name	Sequence (5′→3′)
D1	GAT ATG AGC GAT GTT GTC TT
D2	TTG TCT TCC CAC CCA TGT TAC TCT
H1	SH-CTG GAC GAT ATG CCG ATT GAG AAG GTG CAT ATC
H2	ATT CTG GAC ACA AGA GTA TrAG CAT ATC GTC CAG
H3	Acrydite-TGG TAG GTC AAG GTG CAT ATG GAT GTT AGA GAT ATG CAC CTT CTC AAT CG
H4	TCT AAC ATC CAT ATG CAC GCG ATT GAG AAG GTG CAT ATG GAG TCT AAT CGG CGG GTA AA
A1	Acrydite-TTT ACC CGC CGA TTA GAC

(Note: The same color portion and the underlined sequences indicate that these sequences are complementary to each other. The double underlined sequences represent same bases. The red portion refers to ribonuclease-modified site.)

Table 2. Recovery experiments of the proposed biosensor in drinking water samples (n = 3).

Samples	Hg^{2+} spiked (M)	Hg^{2+} recovered (M)	Recovery (%)	RSD (%)
1	2×10^{-12}	1.904×10^{-12}	95.2	3.2
2	2×10^{-11}	2.025×10^{-11}	101.3	6.8
3	2×10^{-10}	2.047×10^{-10}	102.4	4.8
4	5×10^{-10}	4.904×10^{-10}	98.1	5.1
5	1×10^{-9}	1.033×10^{-10}	103.3	6.5

Highlights

- Monitoring Hg^{2+} by utilizing DNA hydrogel as electrochemical signal amplification element.
- Incorporating T-Hg^{2+}-T into Mg^{2+}-DNAzyme for target cycling amplification.
- Analytical performance of the impedance biosensor is down to picomole level.
- Displaying excellent applicability for evaluating Hg^{2+} in real samples.

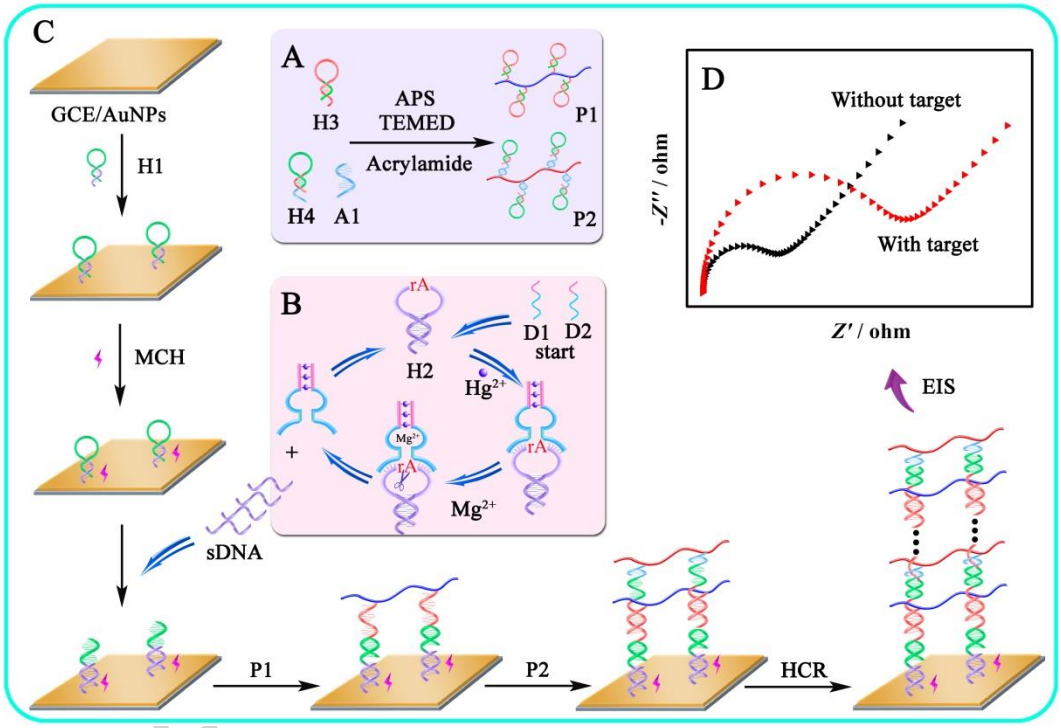

Scheme 1

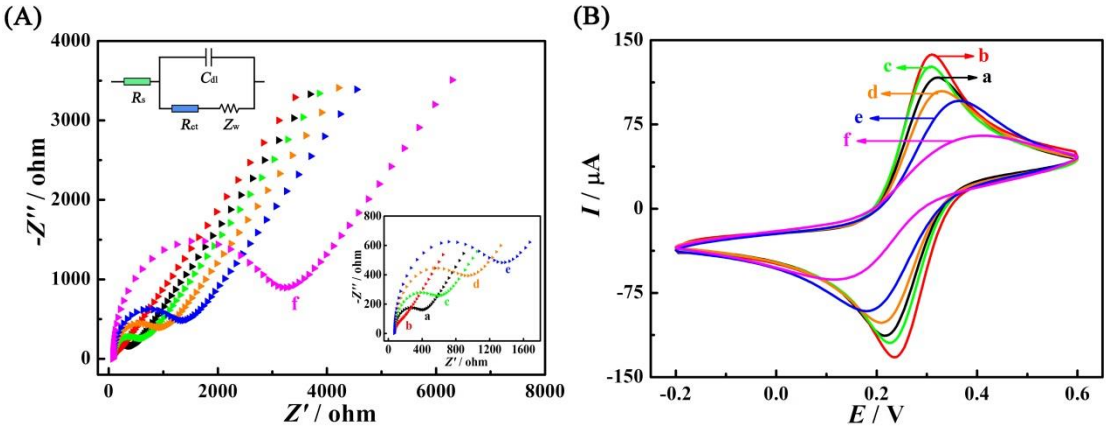

Figure 1

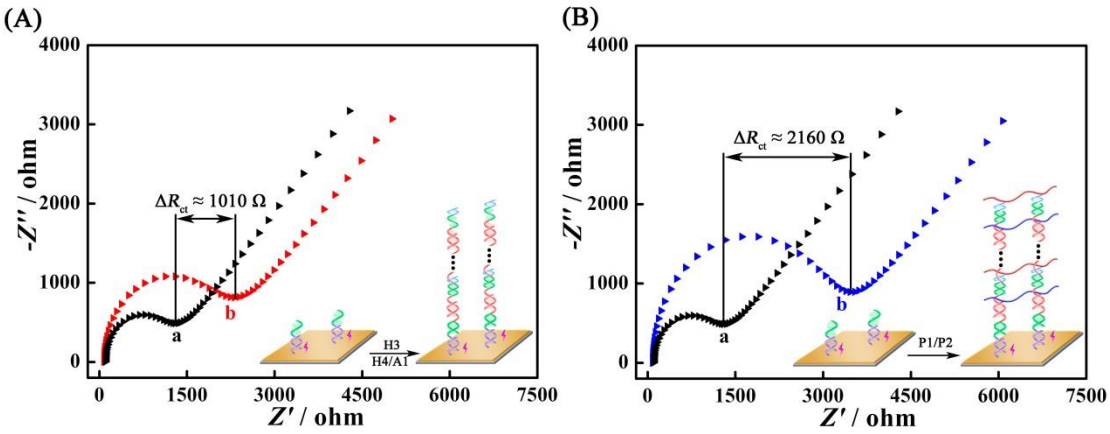

Figure 2

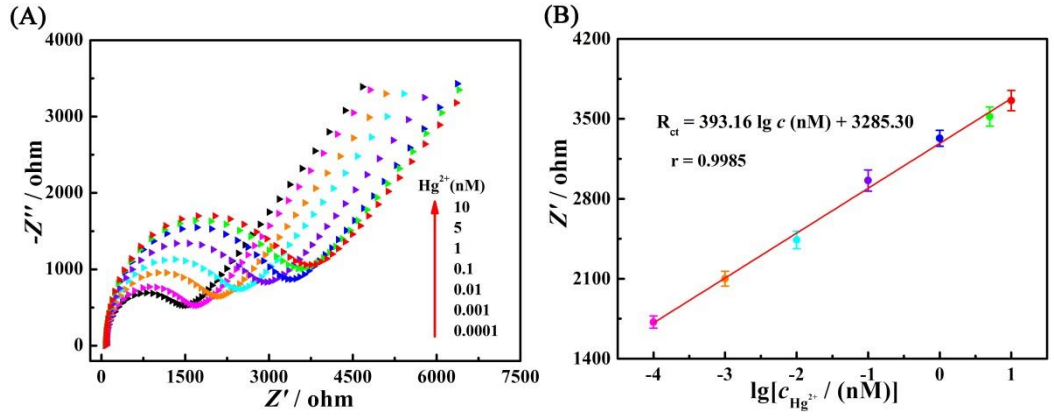

Figure 3

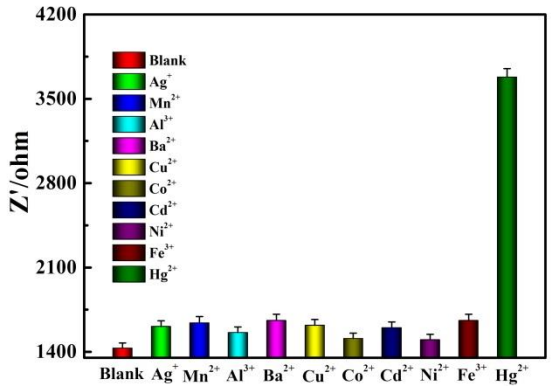

Figure 4